

Quantum Mechanical Model for the Dissociative Adsorption of Diatomic Molecules on Metal Surfaces

Ernst D. German,^{*,†} Alexander M. Kuznetsov,[‡] and Moshe Sheintuch[†]

Department of Chemical Engineering, Technion-Israel Institute of Technology, Haifa 32000, Israel, and
Institute of Electrochemistry of the Russian Academy of Sciences, Leninskii Prospekt 31,
117071 Moscow Russia

Received: December 9, 2004; In Final Form: February 17, 2005

A quantum mechanical nonadiabatic theory of dissociative adsorption of diatomic molecules X_2 on metal surface is presented. The following reaction coordinates are used to construct crossing diabatic potential energy surfaces (PES): the distance y between the atoms of the X_2 molecule, the distance x of the X_2 molecular axis from the surface, the set of coordinates describing possible displacements of metal atoms under adsorption. Expression for the rate constant is derived using the model potentials describing vibrations along these coordinates. The calculated dependency of the rate constant W on the reaction heat ΔE is compared with that in classical approximation. It is shown that quantum effects lead to a weaker dependence of W on ΔE as compared to that for classical one.

1. Introduction

A number of models for calculations of the rate constants for adiabatic and nonadiabatic processes of dissociative adsorption of diatomic molecules at metals have been suggested over the past decade. A method of effective Hamiltonian for calculation of the activation energy was worked out in ref 1. These authors constructed the adiabatic potential energy surfaces (PES) for the dissociative adsorption at metal electrodes using Schmickler's theory² of electrochemical reactions and considering the motion along three reactive modes. An approach for nonadiabatic dissociative adsorption of homonuclear diatomic molecules taking into account the structural reorganization of the surface and the solvent effect was developed.^{3,4} The coordinates that characterize the molecular vibrations of the substrate, as well as coordinates describing the state of the solvent in the case of catalytic reactions at the solid/liquid interface, were introduced into the theoretical model in addition to coordinates of adsorbate molecules. The motion along all these coordinates was supposed to be classical. A model for the calculation of the transition state on the adiabatic potential energy surface for the process of the dissociative adsorption was presented in refs 5 and 6.

The classical description of the motion along all reactive modes, however, seems not to be always valid for the processes under discussion. Specifically, the O–O vibration frequency of molecular oxygen adsorbed on different metals may reach $\sim 1000\text{ cm}^{-1}$ for the “ontop” and “onbond” adsorption positions.⁶ If the dissociative adsorption of nitrogen or hydrogen is considered, the frequency is apparently much higher than that for oxygen. One may expect that the motion along this mode will have a quantum character. We note that a tunneling mechanism has gained popularity several years ago to describe the mechanism of oxygen dissociative adsorption on silver surfaces.^{7–9} Therefore, a modified model is needed where

possible quantum effects were incorporated. This is the subject of the present paper where the process of dissociative adsorption of a homonuclear molecule with one quantum degree of freedom is considered in terms of nonadiabatic theory. A model and first results are presented.

Generally speaking, there appears to be little justification for taking the nonadiabatic approach to consider the dissociative adsorption since this process is usually not electronically nonadiabatic. Nonadiabatic effects for this reaction are usually limited to electron–hole pair excitation or spin-conservation effects which are not part of this model. Nevertheless, the nonadiabatic approach is useful to compare quantum and classical results. As was shown in ref 3, results for an adiabatic case may be obtained from a nonadiabatic one by means of correction of the activation energy using known approximate expression.¹⁰ The correctness of this approximation was particularly confirmed in ref 5 where it was shown that the coordinates of transition states calculated in the nonadiabatic model may be very close to those calculated in the adiabatic model. At last we note, that for number of dissociative reactions (for example, for oxygen dissociative adsorption) the transition state is close to the initial one. Because of this fact, the resonance splitting in the transition state that depends on reaction coordinates may be rather small.³

2. Theoretical Model

According to a generally accepted point of view,^{7,11} one of the mechanisms of dissociative adsorption of an X_2 molecule on transition metals is described by a two-step process. The first step is the nonactivated formation of the stable molecularly adsorbed complex (precursor) between X_2 and a metal surface



where a “star” denotes that the X–X bond is somewhat stretched compared to that in a free molecule, due to a partial charge transfer from the metal to the molecule. The second step is the activated transition of the precursor to the atomic adsorbed

* Corresponding author. E-mail address: ernst_german@yahoo.com.

† Technion-Israel Institute of Technology.

‡ Russian Academy of Sciences.

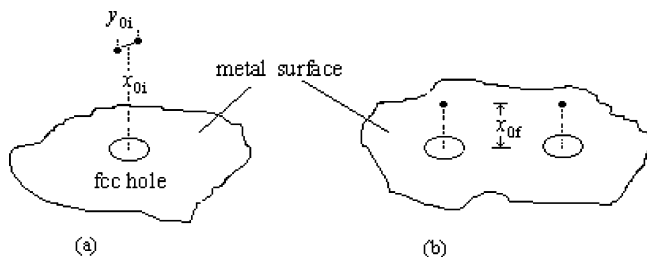
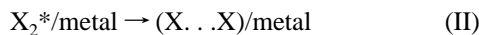


Figure 1. Pictorial view of a diatomic molecule dissociative adsorption on a "hole" position of a metal surface.

(final) state when the X–X bond is disrupted, and the X atoms approach the metal surface at a shorter distance



In this paper we consider only reaction II, and our goal is to calculate the rate constant of formation of the dissociated state $(\text{X} \dots \text{X})/\text{metal}$ from the precursor $\text{X}_2^*/\text{metal}$. This reaction is obviously the rate-determining step of the above mechanism.

(a) Potential Surfaces. We assume the X_2 molecule to be in a position parallel to the metal (Figure 1).^{5,6} The initial, U_i , and final, U_f , potential energy surfaces (PES) are introduced to describe step II. Each of these potential surfaces represents the total energy of the whole system that depends on a set of coordinates $\{r_k\}$ describing the vibrations of the metal nuclei, on the distance x between the center of mass of X_2 and the metal surface, and on the coordinate y describing the intramolecular vibrations of the X_2 molecule. The symbol X_2 is used here as a general notation of the reactant in the undissociated and dissociated state.

The simplest form of U_i and U_f is that obtained under the assumption that the vibration modes along the coordinates x , y , and $\{r_k\}$ are not coupled. In this case, both potential surfaces may be written as a sum of three separate components. One, $v(x)$, characterizes the interaction between X_2 and a metal surface in the direction perpendicular to the surface. The second, $u(y)$, is the vibration for X_2 . The third term, $w(\{r_k\})$, is due to the vibrations of the metal atoms. Thus, providing these components with the subscripts "i" and "f", we have

$$U_i(x, y, \{r_k\}) = w_i(\{r_k\}) + u_i(y) + v_i(x) \quad (1)$$

$$U_f(x, y, \{r_k\}) = w_f(\{r_k\}) + u_f(y) + v_f(x) + \Delta J \quad (2)$$

Here ΔJ is the difference of the energy values at the minima of the potential energy surfaces of the final and initial states. The minimum energy of the initial state is taken to be zero.

We describe now the assumed forms of the functions $v(x)$, $u(y)$ and $w(\{r_k\})$. The potential energies $w_i(\{r_k\})$ and $w_f(\{r_k\})$ are usually written in harmonic approximation since metal atoms perform small vibrations in the crystal lattice; these potential energies are represented as the sum of the harmonic potentials of a set of independent oscillators

$$w_i(\{r_k\}) = \frac{1}{2} \sum_k m \omega_k^2 r_k^2 \quad (3)$$

$$w_f(\{r_k\}) = \frac{1}{2} \sum_k m \omega_k^2 (r_k - \Delta r_{k0})^2 \quad (4)$$

where $\Delta r_{k0} = r_{k0f} - r_{k0i}$, ω_k is the vibration frequency, and m is the reduced mass.

The interaction potential of the adsorbate molecule with the surface, $v_i(x)$, includes effects of the interaction of its HOMO

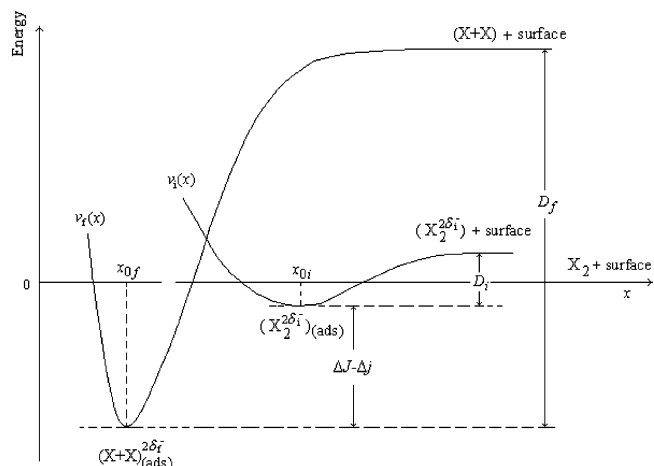


Figure 2. Morse potential energy curves along the x coordinate that illustrates molecular and dissociative adsorbed states of a X_2 molecule; x_{0i} and x_{0f} are the initial and the final equilibrium distances of X_2 from the surface; ΔE is the reaction energy, ΔE_i and ΔE_f are the corresponding adsorption heats, D_i and D_f are the dissociative parameters of the initial and final Morse curves.

with the metal electronic levels, van der Waals attraction, Pauli repulsion, etc. According to our quantum chemical calculations for various clusters⁶ it has a Morse form

$$v_i(x) = D_i [1 - e^{-\beta_i(x-x_{0i})}]^2 \quad (5)$$

The interaction potential of the dissociated system $\text{X} \dots \text{X}$ with the surface, $v_f(x)$, characterizes the interaction of two X atoms with the surface. The motion of two atoms along the x -axis in the dissociated state in general should be described by two degrees of freedom. However, in the classical limit and in view of the symmetry of this system it is sufficient to consider only "synchronous" shift of both atoms to or from the metal surface. One coordinate x is sufficient then for the description of their potential energy. The latter will be approximate also by the Morse function⁶

$$v_f(x) = D_f [1 - e^{-\beta_f(x-x_{0f})}]^2 \quad (6)$$

These curves are shown in Figure 2. In eqs 5 and 6, β_i and β_f are the anharmonicity constants equal to⁶

$$\beta_{i,f} = \sqrt{M(\omega_{i,f}^x)^2 / 2D_{i,f}}$$

where M is the corresponding reduced mass, $\omega_{i,f}^x$ is the frequency, and $D_{i,f}$ is the depth of the potential well (see Figure 2).

The function $u_i(y)$ is the potential energy of nondissociated adsorbed molecule X_2 . Therefore, the Morse-form approximation seems to be appropriate

$$u_i(y) = B_i [1 - e^{-\alpha_i(y-y_{0i})}]^2 \quad (7)$$

where the anharmonicity constant⁶

$$\alpha_i = \sqrt{\mu(\omega_i^y)^2 / 2B_i}$$

depends on the corresponding reduced mass μ , the vibration frequency ω_i^y , and the dissociation energy B_i (see Figure 3).

The interaction between the dissociated fragments X (in the final state) is assumed to have a repulsive character up to long

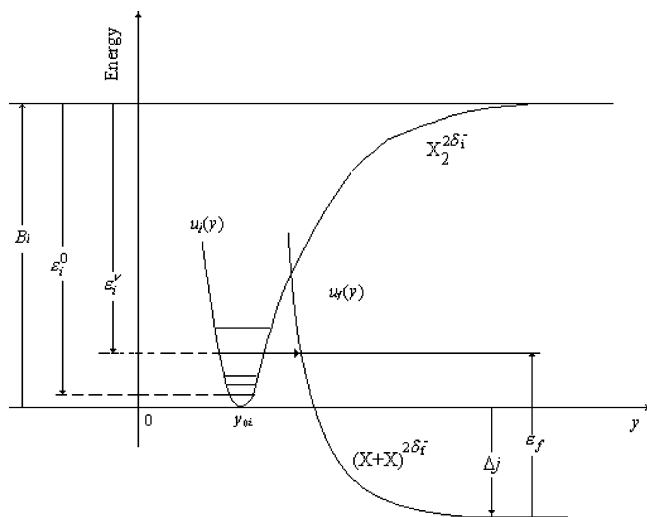


Figure 3. Morse/exponential potentials along the y coordinate describing the molecular adsorbed and dissociated states; B_i is the dissociation parameter of the potential curve u_i ; Δj is the energy of transition along the coordinate y .

distances and is described by the exponential function

$$u_f(y) = B_i e^{-2\alpha_f(y-y_{0i})} + \Delta j \quad (8)$$

where Δj characterizes the position of the curve u_f relative to the y axis as shown in Figure 3.

(b) Transition Probability. According to the aforesaid, we need to calculate the rate constant of step II, i.e., the average transition probability per unit time from the potential surface U_i to the potential surface U_f . The most appropriate method for nonadiabatic reactions (which is rigorous at small interaction V between the reactants) is the Fermi Golden Rule.^{10,12,13} Let us introduce the wave functions of the initial and final states using the Born–Oppenheimer approximation¹²

$$\Psi_i^{\nu, m_k} = \varphi_i(R; y, \{r_k\}) \chi_i^\nu(y) \prod_k \phi_i^{m_k}(r_k) \quad (9)$$

$$\Psi_f^{\epsilon_f, m_k} = \varphi_f(R; y, \{r_k\}) \chi_f^{\epsilon_f}(y) \prod_k \phi_f^{m_k}(r_k) \quad (10)$$

Here $\varphi_{i,f}$ are the electronic wave functions and R is the electronic coordinate, $\chi_{i,f}$ are the nuclear wave functions describing a relative motion of X atoms along the quantum degree of freedom y . The function χ_i^ν is characterized by the quantum vibration number ν , and the function $\chi_f^{\epsilon_f}$ corresponds to the energy level ϵ_f in a continuous manifold of energies of the final decaying potential $u_f(y)$. The $\phi_i^{m_k}(r_k)$ and $\phi_f^{m_k}(r_k)$ terms are the wave functions of the phonon subsystem in the initial vibration state n_k and the final vibration state m_k , respectively. The total energies of the whole system including the energies $v_{i,f}(x)$ of the classical subsystem are equal to

$$E_i^{n_k, \nu} = \sum_k \hbar \omega_k (n_k + 1/2) + B_i - \epsilon_i^\nu + v_i(x) \quad (11)$$

$$E_i^{m_k, \epsilon_f} = \sum_k \hbar \omega_k (m_k + 1/2) + \epsilon_f + v_f(x) + \Delta j \quad (12)$$

The energy levels ϵ_i^ν in the Morse potential well (eq 7) are given by equation¹²

$$\epsilon_i^\nu = B_i \left[1 - \frac{\alpha_i \hbar}{\sqrt{2\mu B_i}} (\nu + 1/2) \right]^2 \quad (13)$$

Note that energy levels ϵ_i^ν start from the energy $u_i(y)$ at infinity, i.e., from the energy value equal to B_i (see Figure 3). Therefore, the energy distance of the level ϵ_i^ν from y -axis in Figure 3 is equal to $B_i - \epsilon_i^\nu$. The energy levels ϵ_f start from the value of the $u_f(y)$ at infinity. Since according to eq 8 $u_f(\infty) = \Delta j$, we can see from Figure 3 that under the conditions of the Franck–Condon principle for the quantum subsystem¹²

$$\epsilon_f = B_i - \epsilon_i^\nu - \Delta j \quad (14)$$

where $\Delta j < 0$ if the value of $u_f(\infty)$ is negative, and $\Delta j > 0$ if $u_f(\infty) > 0$.

First, we calculate the average probability of the transition (per unit time) from the initial state to the final state at the fixed distance x . In Condon approximation it may be presented in the following form (see Appendix A):

$$P(x) = \frac{V^2}{i\hbar k_B T} \times \sum_{\nu=0}^{\infty} \exp[-(\epsilon_i^0 - \epsilon_i^\nu)/k_B T] \int_0^\infty d\epsilon_f \rho(\epsilon_f) \frac{c \exp[-\sigma(\nu, \epsilon_f)]}{Z_y} \times \int_{-\infty}^{i\infty} d\theta \exp[-\{\theta \Delta I + \theta(1-\theta)E_r + \theta[v_f(x) - v_i(x)]\}/k_B T] \quad (15)$$

where the notation

$$|\langle \chi_f^{\epsilon_f}(y) | \chi_i^\nu(y) \rangle|^2 \equiv c e^{-\sigma(\nu, \epsilon_f)} \quad (16)$$

of the square of the overlap integral of the wave functions for the quantum degree of freedom was introduced, and ΔI is given by eq A10. The constant c in eqs 15 and 16 is due to the normalization of the wave functions $\chi_{i,f}(y)$ (for details see Appendix B). Equation 15 determines the probability of the transition at fixed value of the coordinate x . The total transition probability W is obtained by the weighted integration of $P(x)$ over x

$$W = \frac{1}{Z_x} \int_0^\infty e^{-[v_i(x)/k_B T]} P(x) dx = \int_0^\infty dx \frac{V^2}{i\hbar k_B T} \sum_{\nu} \exp[-(\epsilon_i^0 - \epsilon_i^\nu)/k_B T] \int_0^\infty d\epsilon_f \rho(\epsilon_f) \times \frac{c \exp[-\sigma(\nu, \epsilon_f)]}{Z_y} \times \int_{-\infty}^{i\infty} d\theta \exp[-\{\theta \Delta I + \theta(1-\theta)E_r\}/k_B T] \times \frac{1}{Z_x} \int_0^\infty dx \exp[-\{\theta v_f(x) + (1-\theta)v_i(x)\}/k_B T] \quad (17)$$

where Z_x is the configurational integral.

The integrals over x and θ can be calculated approximately using the saddle point method.^{10,13} The calculation leads to the following equation for the transition probability:

$$W = \frac{V^2}{\hbar k_B T} \sum_{\nu} e^{-(\epsilon_i^0 - \epsilon_i^{\nu})/k_B T} \int_0^{\infty} d\epsilon_f \rho(\epsilon_f) \times \sqrt{\frac{2\pi k_B T (v_i'')_{x_{0i}}}{|H''(\hat{\theta}, \hat{x})| f''(\hat{\theta}, \hat{x})}} \frac{c \exp[-\sigma(\nu, \epsilon_f)]}{Z_y} \exp[-H(\hat{\theta}, \hat{x})/k_B T] \quad (18)$$

where \hat{x} and $\hat{\theta}$ are the coordinates of the saddle point determined by the equations

$$(1 - \theta) \frac{dv_i(x)}{dx} + \theta \frac{dv_f(x)}{dx} = 0 \quad (19)$$

$$\Delta I + v_f(\hat{x}) - v_i(\hat{x}) + (1 - 2\theta)E_r = 0 \quad (20)$$

In eq 18, $f''(\hat{x}) = (\partial^2 f / \partial x^2)_{\hat{x}}$ is the partial second derivative of the function

$$f(x) = \theta v_f(x) + (1 - \theta)v_i(x) \quad (21)$$

with respect to x , $H''(\hat{x}, \hat{\theta}) = (d^2 H / d\theta^2)_{\hat{\theta}}$ is the total second derivative of the function

$$H(\theta, x) = \theta(\Delta I - \Delta j) + f(x) + \theta(1 - \theta)E_r \quad (22)$$

with respect to θ , and $v_i''(x)_{x_{0i}}$ is the second derivative of the function $v_i(x)$ with respect to x . The product $f''(\hat{x}, \hat{\theta}) \cdot |H''(\hat{\theta}, \hat{x})|$ may be represented in the following form suitable for the numerical calculation¹³

$$\Gamma(\hat{x}, \hat{\theta}) = f''(\hat{x}, \hat{\theta}) |H''(\hat{\theta}, \hat{x})| = [\Delta I - \Delta j + E_r + v_f(x) - v_i(\hat{x})][v_f''(\hat{x}) - v_i''(\hat{x})] + 2v_i'(\hat{x})E_r + [v_i'(\hat{x}) - v_f'(\hat{x})]^2 \quad (23)$$

(for determination of the derivatives see Appendix C). A more compact form for $H(x, \theta)$ emerges with the use of eq 20:

$$H(x, \theta) = v_i(x) + \theta^2 E_r \quad (24)$$

Equations 18–20 may be used for numerical calculations; however, since the calculation of the matrix element (eq 16) is rather difficult, we transform eq 18 into a more convenient form for the application of a quasi-classical approximation.¹² The physical meaning of eq 18 is the following. The transition between two energy levels ϵ_i^{ν} and ϵ_f corresponds to the transition along the classical coordinates x and $\{r_k\}$ with the effective energy of transition equal to $\Delta I = \Delta J - \Delta j$ where $\Delta j = B_i - \epsilon_i^{\nu} - \epsilon_f$ (see eq 14). Since the total reaction energy is equal to ΔJ , the energy of transition along the coordinate y is Δj (Figure 3). Different ϵ_f values correspond to different Δj . Therefore, for a given ν the integration over ϵ_f is equivalent to the integration over Δj :

$$W = \frac{V^2}{\hbar k_B T} \sum_{\nu} e^{-(\epsilon_i^0 - \epsilon_i^{\nu})/k_B T} \times \int_{-\infty}^{B_i - \epsilon_i^{\nu}} d\Delta j \rho(\Delta j) \sqrt{\frac{2\pi k_B T (v_i'')_{x_{0i}}}{\Gamma(\hat{\theta}, \hat{x})}} \frac{c e^{-\sigma(\nu, \Delta j)}}{Z_y} e^{-(\hat{v}_i + \hat{\theta}^2 E_r)/k_B T} \quad (25)$$

where \hat{v}_i is the value of the potential $v_i(x)$ at the transition configuration \hat{x} . Note that, according to eqs 19 and 20, \hat{v}_i and $\hat{\theta}$ depend on Δj .

Let us transform eq 25 using eqs 19 and 20 as follows. We have from eq 19 that

$$\theta = \frac{\partial v_i(x)/\partial x}{\partial v_i(x)/\partial x - \partial v_f(x)/\partial x} \quad (26)$$

Substitution of eq 26 into eq 20 allows deriving the energy Δj as function of \hat{x} :

$$\Delta j = \Delta I + v_f(\hat{x}) - v_i(\hat{x}) - E_r \frac{\partial v_i(\hat{x})/\partial x + \partial v_f(\hat{x})/\partial x}{\partial v_i(\hat{x})/\partial x - \partial v_f(\hat{x})/\partial x} \quad (27)$$

Now, one can replace the integration over Δj in eq 25 by the integration over \hat{x} using eq 27,¹³ i.e.,

$$W = \frac{V^2}{\hbar k_B T} \sum_{\nu} \int d\hat{x} \times \left(\frac{\partial \Delta j}{\partial \hat{x}} \right) \rho(\Delta j) \sqrt{\frac{2\pi k_B T (v_i'')_{x_{0i}}}{\Gamma(\hat{\theta}, \hat{x})}} \frac{c e^{-\sigma(\nu, \hat{x})}}{Z_y} \exp[-E_a^{\nu}(\hat{x})/k_B T] \quad (28)$$

where the partial activation energy E_a^{ν} is equal to

$$E_a^{\nu}(\hat{x}) = \epsilon_i^0 - \epsilon_i^{\nu} + v_i(\hat{x}) + \left(\frac{v_i'(\hat{x})}{v_i'(\hat{x}) - v_f'(\hat{x})} \right)^2 E_r \quad (29)$$

Here prime denotes the first derivative of the functions v_i and v_f with respect to \hat{x} . The integration limits in eq 28 are determined by the mutual disposition of the curves u_i and u_f (see Figure 3) since, due to eq 27, the change of \hat{x} leads to the change of Δj , i.e., to the shift of the curve u_f relative to the curve u_i (see Appendix B). The lower limit is given by the value of \hat{x} at the crossing point of the curves u_i and u_f that coincides with the crossing point of the level ν and the curve $u_i(y)$. The upper integration limit is given by such value \hat{x} at that the level \hat{v}_i is tangential to curve u_f .

The exponent $\sigma(\nu)$ sharply increases and E_a^{ν} decreases when \hat{x} varies from the lower to the upper integration limit, i.e., the product $e^{-\sigma(\nu)} e^{-E_a^{\nu}/k_B T}$ has a sharp maximum within the integration region. Other terms of the integrand in eq 28 are smooth functions of \hat{x} . Therefore, we can approximately calculate the integral over \hat{x} , taking the slowly changing functions out of the integral at the point of maximum of integrand and extending formally the integration limits from $-\infty$ to ∞ . Then using the saddle point method we obtain

$$W = \frac{V^2}{\hbar k_B T} \sum_{\nu} c \rho(\hat{x}^*) \left(\frac{d\Delta j}{d\hat{x}} \right)_{\hat{x}^*} \sqrt{\frac{2\pi k_B T (v_i'')_{x_{0i}}}{\Gamma(\hat{x}^*, \hat{\theta})}} \times \sqrt{\frac{2\pi k_B T}{(\psi'')_{\hat{x}^*}}} \frac{e^{-\sigma(\nu, \hat{x}^*)}}{Z_y} e^{-E_a^{\nu}(\hat{x}^*)/k_B T} \quad (30)$$

where ψ'' is the second derivative of the function $\psi = k_B T \sigma(\hat{x}) + E_a^{\nu}(\hat{x})$ with respect to \hat{x} , and the coordinate of the saddle point \hat{x}^* is determined by equation

$$k_B T \frac{d\sigma}{d\hat{x}} + \frac{dE_a^{\nu}}{d\hat{x}} = 0 \quad (31)$$

A more detailed numerical analysis shows that the approximate integration over x in eq 30 gives the upper estimation of this integral, overestimating the value of the rate constant about by 1.5–2 times. This is due to the fact that the integrand $e^{-\sigma(\nu)} e^{-E_a^{\nu}/k_B T}$ actually has the form of partial Gaussian curve

TABLE 1: Parameters Used for Numerical Calculations⁶

item	value	item	value
$\Delta E_i/\text{kcal/mol}$	-8.5	$y_{0i}/\text{\AA}$	1.395
$\Delta E_f/\text{kcal/mol}$	-54	$B_i/\text{kcal/mol}$	80
$\omega_i^x/\text{cm}^{-1}$	395	$B_f/\text{kcal/mol}$	24
$\omega_i^y/\text{cm}^{-1}$	490	$D_i/\text{kcal/mol}$	19.5
$\omega_i^z/\text{cm}^{-1}$	850	$D_f/\text{kcal/mol}$	174
$x_{0i}/\text{\AA}$	1.70	$V/\text{kcal/mol}$	0.6
$x_{0f}/\text{\AA}$	1.16	$E_f/\text{kcal/mol}$	4

because of the truncation of the integration interval over \hat{x} to the left of the maximum, which is determined by the limits of integration in eq 29. To take this fact into account, a constant Λ is introduced into eq 30 which values range between 0.5 and 1. Finally, we represent eq 30 in the following form:

$$W = \sum_{\nu=0} A_{\nu} e^{-\sigma(\nu, \hat{x}^*)} e^{-E_a^{\nu}(\hat{x}^*)/k_B T} \quad (32a)$$

$$A_{\nu} = \Lambda \frac{2\pi V^2}{\hbar Z_y} c \rho_{\nu} \left(\frac{d\Delta j}{d\hat{x}} \right)_{\hat{x}^*} \sqrt{\frac{(v_i'')_{x_{0i}}}{\Gamma(\hat{x}^*, \hat{\theta}) \psi''_{\hat{x}^*}}} \quad (32b)$$

Note that the quantity $\Delta J = \Delta I + \Delta j$ (see eq A10) that is involved in eqs 20, 22, and 23, and other equations differs from the thermodynamic reaction heat ΔE by the difference of the energies of the zero-point vibrations of the final and initial states. In our case $\Delta E = \Delta J - \epsilon_i^0$ since the ground level in the continuous manifold of energies in the decaying potential $u_f(y)$ was accepted to be equal to zero. Therefore in the further discussion we substitute ΔJ by ΔE and eq A10 by $\Delta I = \Delta E + \Delta j$, neglecting the small difference between these quantities for simplicity.

3. Discussion

Equations 29 and 32 represent one of the main results of the paper. They allow us to estimate the transition probability (rate constant) for the dissociative adsorption of diatomic molecules on metal surfaces with due account of quantum effects given by the factor $e^{-\sigma}$. The kinetic characteristics of reactions that emerge from these equations in general differ from these corresponding to the purely classical limit for the chemical bond X–X. The activation barrier in the quantum case is independent of the dissociation energy B_i of the molecule X_2 at a fixed value of the reaction heat ΔE . The effect of B_i on the rate constant (W) is implicitly represented by eq 29 for the tunneling factor $e^{-\sigma}$. Due to this factor, the rate constant of the oxygen dissociative adsorption is mass sensitive and a difference between $^{16}\text{O}_2$ and $^{18}\text{O}_2$ might be observed.

If the molecular potential $u_i(y)$ is sufficiently steep, one may expect that the major contribution to the sum over ν in eq 32 comes from the term with $\nu = 0$, i.e., the ground vibration state of the molecule X_2 mainly participates in the transition that leads to the dissociative adsorption. In this limit we may approximately restrict ourselves by one term in eq 32 with $\nu = 0$.

This general analysis is confirmed by numerical calculations given below. As an example, we calculate the rate constant W using the parameters of the Morse and exponential potentials for oxygen adsorption on Pd(111) surface. These parameters taken from ref 6 are listed in Table 1 where ΔE_i and ΔE_f are the adsorption energies for the molecular adsorbed and dissociated states (Figure 2), and $\Delta E = \Delta E_f - \Delta E_i$. The anharmonicity constant α_f in eq 8 is taken to be equal to α_i in eq 7.⁶

The results of the quadratic approximations of the partial activation energy and tunneling factor are given in Table 2 for

TABLE 2: Coefficients of Equation $\varphi = aY^2 + bY + c$ (where $Y = \sigma(\nu)$ or E_a^{ν}) Calculated at $\Delta E = -45.5$ kcal/mol; $T = 298$ K

no. of energy level ν	$\sigma(\nu)$			$E_a^{\nu a}$		
	a	-b	c	a	-b	c
0	1851	5928	4744	464	1564	1318
1	2154	6974	5645	400	1353	1146
2	2343	7656	6255	363	1229	1044
3	2739	9039	7458	347	1176	1001
4	3082	10261	8540	319	1083	924

^a E_a^{ν} in kcal/mol.

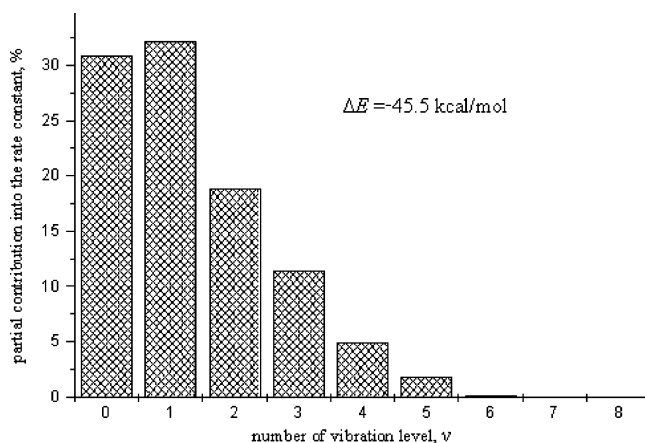


Figure 4. Partial contributions (%) to the rate constant W of the transitions from vibration energy levels ϵ_i^{ν} of the O–O bond into the continuous manifold of energy levels of the decay potential; reaction energy $\Delta E = -45.5$ kcal/mol, $T = 298$ K.

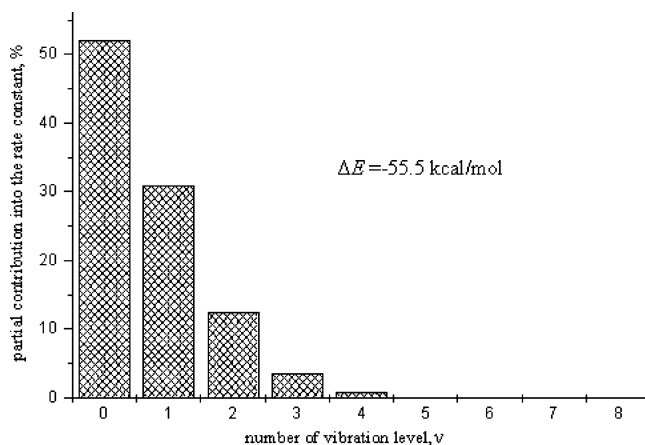


Figure 5. Partial contributions (%) to the rate constant W of the transitions from vibration energy levels ϵ_i^{ν} of the O–O bond into the continuous manifold of energy levels of the decay potential; reaction energy $\Delta E = -55.5$ kcal/mol, $T = 298$ K.

several low-lying energy levels. Using data of Tables 1 and 2 we calculated the contribution of the transitions from different vibration energy levels of the O–O bond to the rate constant W (Figure 4) for oxygen adsorption on Pd(111) characterized by $\Delta E = -45.5$. Similar calculations were also performed for reactions characterized by a more negative ($\Delta E = -55.5$ kcal/mol) and a more positive ($\Delta E = -35.5$ kcal/mol) value. These ΔE values were obtained by means of changing the value of ΔE_f at fixed values of other parameters except D_f , which depends on the value of ΔE .⁶ The results are shown in Figures 5 and 6.

One can see that at $\Delta E = -55.5$ kcal/mol (Figure 5) the transition along the y coordinate occurs mainly by means of tunneling from the ground and first excited vibration states of

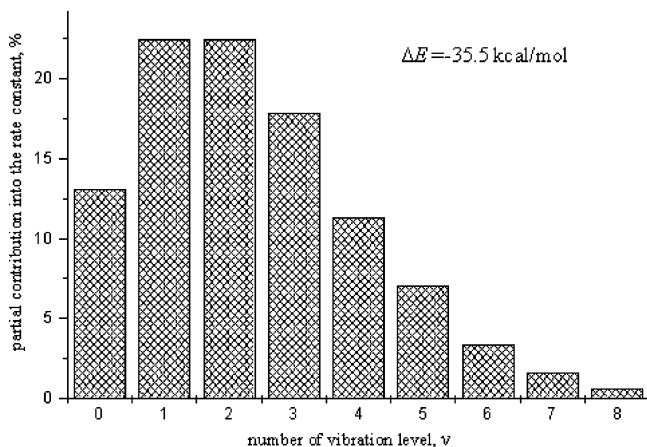


Figure 6. Partial contributions (%) to the rate constant W of the transitions from vibration energy levels ϵ_i^ν of the O–O bond into the continuous manifold of energy levels of the decay potential; reaction energy $\Delta E = -35.5$ kcal/mol, $T = 298$ K.

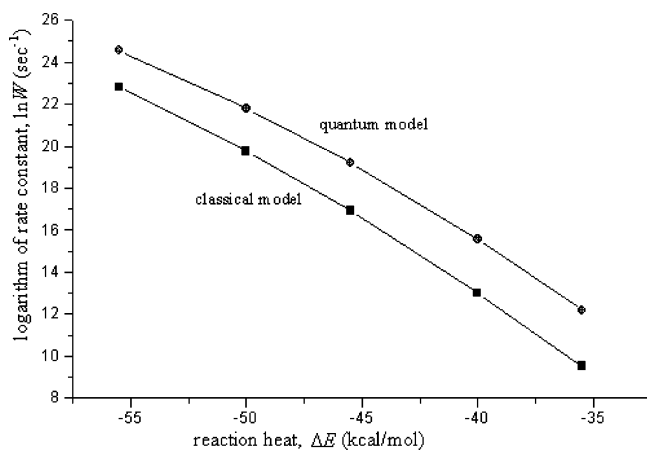


Figure 7. Comparison of the correlations between logarithm of the rate constant of the oxygen dissociative adsorption and the reaction energy calculated in the classical and quantum models.

O_2 molecule ($\nu = 0, 1$) to the continuum of the energy levels of the final exponential potential describing the repulsion of oxygen atoms. For a less exothermic reaction (at $\Delta E = -35.5$, Figure 6) a greater number of the initial vibration states take part in the transition. The major contribution to the transition probability comes from the energy levels with $\nu = 1, 2, 0$, and 3. It corresponds to a greater (on average) elongation of the O–O bond, i.e., to a more classical behavior.

The dependence of the quantum effects on the reaction energy ΔE is reflected also in the Brønsted plots $\ln W$ vs ΔE (Figure 7). This figure shows that curve 1 calculated under the assumption of quantum motion along the y coordinate and curve 2 calculated in the classical model³ diverge in the region of less negative reaction heats where the contribution of the excited states is of importance.

4. Conclusions

A quantum mechanical nonadiabatic theory of the dissociative adsorption of diatomic molecules X_2 on metal surfaces is presented. An approximate expression for the rate constant is derived (eqs 40 and 43) for the model potentials describing the interaction of the X_2 with a metal surface, and the interaction of X atoms with each other. Numerical estimations are performed using the parameters of the oxygen dissociative adsorption on Pd(111) surface. The relative contributions of the

transitions from different vibration energy levels to the total transition probability W are calculated. The results show that for metals characterized by larger negative reaction heats of dissociative adsorption and therefore by lower activation barriers, the tunneling plays a lower role than that for metals with the higher activation barriers. This should lead to a stronger temperature dependence of the dissociative sticking probability for the former. The dependence of the $\ln W$ on the reaction heat ΔE obtained in quantum model is compared with that calculated in the classical theory. It is shown that the quantum effects lead to a weaker dependence of $\ln W$ on ΔE as compared to the classical one.

Acknowledgment. M.S. and E.G. thank the Grand Water Research Institute for financial support. A.M.K. thanks the Russian Foundation for Basic Research, grant No. 00-03-32239, for partial financial support.

Appendix A

Average Transition Probability at the Fixed Distance x .

In Condon approximation, this probability may be written in the form

$$P(x) = \frac{2\pi}{\hbar} |V_{fi}|^2 \sum_{\nu, m_k, n_k} \int_0^\infty d\epsilon_f \rho(\epsilon_f) \exp[-\tilde{E}_i^{n_k, \nu}/k_B T] \frac{1}{Z_y} |\langle \chi_f^{\epsilon_f} | \chi_i^\nu \rangle|^2 \times \frac{1}{Z_r} \prod_k |\langle \phi_{ik}^{m_k} | \phi_{ik}^{n_k} \rangle|^2 \delta(E_f^{m_k, \epsilon_f} - E_i^{n_k, \nu}) \quad (A1)$$

where $Z_r = \prod_k Z_{r_k}$ is the standard vibration statistical sum for the harmonic potential, the $\tilde{Z}_y = \sum_\nu \exp[-(B_i - \epsilon_i^\nu)/k_B T]$ term is the vibrational statistical sum for the X_2 molecule, $\tilde{E}_i^{n_k, \nu} = E_i^{n_k, \nu} - \nu_i(x) = \sum_k \hbar \omega_k (n_k + 1/2) + B_i - \epsilon_i^\nu$, and the delta-function (δ) is

$$\delta(E_f^{m_k, \epsilon_f} - E_i^{n_k, \nu}) = \frac{1}{2\pi i k_B T} \int_{-i\infty}^{i\infty} d\theta \exp[-\theta(E_f^{m_k, \epsilon_f} - E_i^{n_k, \nu})/k_B T] \quad (A2)$$

is the density of states that, for free one-dimensional motion of a particle with the mass μ , is

$$\rho(\epsilon_f) = \frac{(\mu/2)^{1/2} l}{\pi \hbar (\epsilon_f)^{1/2}} \quad (A3)$$

where l is the length of the normalization “box”, and V_{fi} is the electron resonance integral $V_{fi} = \langle \varphi_f | V | \varphi_i \rangle$. We have after substitution of eq A2 into eq A1

$$P(x) = \frac{V_{fi}^2}{i \hbar k_B T} \sum_{\nu, n_k, m_k} \int_0^\infty d\epsilon_f \rho(\epsilon_f) \int_{-i\infty}^{i\infty} d\theta \times (\tilde{Z}_y)^{-1} |\langle \chi_f^{\epsilon_f} | \chi_i^\nu \rangle|^2 \frac{1}{Z_r} \prod_k |\langle \phi_{ik}^{m_k} | \phi_{ik}^{n_k} \rangle|^2 \exp[-\tilde{E}_i^{n_k, \nu}/k_B T] \exp[-\theta(E_f^{m_k, \epsilon_f} - E_i^{n_k, \nu})/k_B T] \quad (A4)$$

One can transform eq A4 into eq A5 using eqs 11 and 12

$$\begin{aligned}
P(x) = & \frac{V_{fi}^2}{i\hbar k_B T} \sum_{\nu, n_k, m_k} \int_0^\infty d\epsilon_f \rho(\epsilon_f) \int_{-i\infty}^{i\infty} d\theta \times \\
& (\tilde{Z}_y)^{-1} |\langle \chi_f^{\epsilon_f} | \chi_i^\nu \rangle|^2 \prod_k Z_{rk}^{-1} |\langle \phi_{ik}^{m_k} | \phi_{ik}^{n_k} \rangle|^2 \\
& \exp\{-[\sum_k \hbar\omega_k(n_k + 1/2) + B_i - \epsilon_i^\nu]/k_B T\} \\
& \exp\{-\theta[\sum_k \hbar\omega_k m_k - \sum_k \hbar\omega_k n_k]/k_B T\} \\
& \exp\{-\theta[\epsilon_f - B_i + \epsilon_i^\nu + v_f(x) - v_i(x) + \Delta J]/k_B T\} \quad (A5)
\end{aligned}$$

Then we introduce the following notation:

$$\begin{aligned}
\xi_k(\theta) = & \frac{1}{Z_{rk}} \exp\left[-\frac{\hbar\omega_k}{2k_B T}\right] \sum_{n_k, m_k} \exp\left[-\frac{\hbar\omega_k n_k}{k_B T}\right] \\
& \exp\{-\theta[\sum_k \hbar\omega_k m_k - \sum_k \hbar\omega_k n_k]/k_B T\} |\langle \phi_{ik}^{m_k} | \phi_{ik}^{n_k} \rangle|^2 \quad (A6)
\end{aligned}$$

This form was used in ref 3 leading to a compact expression for the product

$$\begin{aligned}
\prod_k \xi_k(\theta) = & \prod_k \exp[-\theta(1 - \theta)E_r/k_B T] = \\
& \exp\left[-\frac{\theta(1 - \theta)E_r}{k_B T}\right] \quad (A7)
\end{aligned}$$

where E_r is the reorganization energy for the classic oscillators.¹⁰ Taking into account eqs A7 and A6, one can rewrite the probability $P(x)$ in the form

$$\begin{aligned}
P(x) = & \frac{V^2}{i\hbar k_B T} \sum_\nu \int_0^\infty d\epsilon_f \rho(\epsilon_f) \tilde{Z}_y^{-1} |\langle \chi_f^{\epsilon_f} | \chi_i^\nu \rangle|^2 \int_{-i\infty}^{i\infty} d\theta \times \\
& \exp[-\theta(1 - \theta)E_r/k_B T] \exp[-(B_i - \epsilon_i^\nu)/k_B T] \\
& \exp[-\theta(\epsilon_f - B_i + \epsilon_i^\nu + v_f(x) - v_i(x) + \Delta J)/k_B T] \quad (A8)
\end{aligned}$$

where $V \equiv V_{fi}$. Let us introduce the following notation

$$\Delta I = \epsilon_f - B_i + \epsilon_i^\nu + \Delta J \quad (A9)$$

which, taking into account eq 14, may be rewritten as

$$\Delta I = \Delta J - \Delta j \quad (A10)$$

We can also transform the term $\exp[-(B_i - \epsilon_i^\nu)/k_B T]/\tilde{Z}_y$ to the equivalent expression $\exp[-(\epsilon_i^0 - \epsilon_i^\nu)/k_B T]/Z_y$, where the statistical sum $Z_y = \sum_\nu e^{-(\epsilon_i^0 - \epsilon_i^\nu)/k_B T}$. Using these notations, eq A8 takes the compact form given by eq 15.

Appendix B

Calculation of the Tunnel Factor. The tunneling factor in eq 14 determined by the overlapping integral (eq 15) is calculated below using the quasi-classical approximation.¹² The quasi-classical wave functions $\chi_i^\nu(y)$ and $\chi_f^{\Delta j}(y)$ are defined as follows

$$\chi_i^\nu = \frac{1}{a^{1/2}} \exp\left[-\frac{1}{\hbar} \int_{y_1}^y dy [2\mu(u_i - B_i + \epsilon_i^\nu)]^{1/2}\right] \quad (B1)$$

$$\chi_f^{\Delta j} = \frac{1}{l^{1/2}} \exp\left[-\frac{1}{\hbar} \int_y^{y_r} dy [2\mu(u_f - B_i + \epsilon_i^\nu + \Delta j)]^{1/2}\right] \quad (B2)$$

where a and l are the normalization constants: a is of the order of the amplitude of zero-point vibrations in the initial well, and l corresponds to normalization of the wave function in the potential ‘‘box’’; y_1 and y_r are the left and right crossing points of the energy level ν with the corresponding potential curves (see Figure 3).

Therefore, we rewrite the overlap integral in the form

$$\begin{aligned}
\langle \chi_i^\nu(y) | \chi_f^{\Delta j}(y) \rangle = & \frac{1}{(al)^{1/2}} \int dy \\
& \exp\left\{-\frac{1}{\hbar} \int_{y_1}^y dy [2\mu(u_i - B_i + \epsilon_i^\nu)]^{1/2} - \frac{1}{\hbar} \times \right. \\
& \left. \int_y^{y_r} dy [2\mu(u_f - B_i + \epsilon_i^\nu + \Delta j)]^{1/2}\right\} \approx c^{1/2} \exp\left\{-\frac{\sqrt{2\mu B_i}}{\hbar} \times \right. \\
& \left. \left[\int_{y_1}^y dy \left[\frac{u_i + \epsilon_i^\nu}{B_i} - 1\right]^{1/2} + \int_y^{y_r} dy \left[\frac{u_f + \epsilon_i^\nu + \Delta j}{B_i} - 1\right]^{1/2} \right]\right\} \quad (B3)
\end{aligned}$$

where $c^{1/2} = \delta y/(al)^{1/2}$, δy is the interval of y values giving the major contribution to the overlap integral, and u_i and u_f are given by eqs 7 and 8. The integration limits in the integrals B3 are as follows.

(1) The low integration limit, y_1 , is the crossing point of the potential curve u_i and the initial energy level $B_i - \epsilon_i^\nu$. We have the following equation:

$$B_i [1 - e^{-\alpha_i(y-y_{0i})}]^2 = B_i - \epsilon_i^\nu \quad (B4)$$

which leads to

$$y_1 = y_{0i} - (1/\alpha_i) \ln[1 - \sqrt{1 - \epsilon_i^\nu/B_i}] \quad (B5)$$

(2) The integration limit \hat{y} is the crossing point of the curves u_i and u_f that is determined by the equation

$$B_i [1 - e^{-\alpha_i(y-y_{0i})}]^2 = B_f e^{-2\alpha_f(y-y_{0f})} + \Delta j \quad (B6)$$

We find from eq B6, assuming $\alpha_i = \alpha_f$, that

$$\hat{y} = y_{0i} - (1/\alpha_i) \ln \frac{1 - \sqrt{1 - (1 - B_f/B_i)(1 - \Delta j/B_i)}}{1 - B_f/B_i} \quad (B7)$$

(3) The upper limit of integration is determined by crossing the of the final curve u_f (with the assumption that $\alpha_i = \alpha_f$) and the energy level $B_i - \epsilon_i^\nu$:

$$B_f e^{-2\alpha_f(y-y_{0f})} + \Delta j = B_i - \epsilon_i^\nu \quad (B8)$$

$$y_r = y_{0f} - (1/2\alpha_f) \ln[(B_i - \epsilon_i^\nu - \Delta j)/B_f] \quad (B9)$$

Appendix C

Differentiation of eqs 5 and 6 leads to the following formulas for the derivatives of these functions used above in eqs for the transition probability:

$$(v_i'')_{x_{0i}} = 2D_i \beta^2 \quad (C1)$$

$$v_{i,f}'(z_{i,f}(x)) = 2D_{i,f} \beta_{i,f} z_{i,f} (1 - z_{i,f}) \quad (C2)$$

$$v_{i,f}''(z_{i,f}(x)) = 2D_{i,f} \beta_{i,f}^2 z_{i,f} (2z_{i,f} - 1) \quad (C3)$$

where

$$z_i(x) = \exp[-\beta_i(x - x_{0i})]$$

and

$$z_f(x) = \exp[-\beta_f(x - x_{0f})]$$

References and Notes

- (1) Koper, M. T. M.; Voth, G. A. *J. Chem. Phys.* **1998**, *109*, 1991.
- (2) Schmickler, W. *J. Electroanal. Chem.* **1979**, *100*, 533.
- (3) German, E. D.; Efremenko, I.; Kuznetsov, A. M.; Sheintuch, M. *J. Phys. Chem. B* **2002**, *106*, 11784.
- (4) German, E. D.; Kuznetsov, A. M.; Efremenko, I. *Russ. J. Electrochem.*, (English ed.) **2003**, *39*, 61.
- (5) German, E. D.; Kuznetsov, A. M. *J. Mol. Struct. (THEOCHEM)* **2004**, *671*, 153.
- (6) German, E. D.; Kuznetsov, A. M.; Sheintuch, M. *Surf. Sci.* **2004**, *554*, 159.
- (7) Nolan, P. D.; Wheeler, M. C.; Davis, J. E.; Mullins, C. B. *Acc. Chem. Res.* **1998**, *31*, 798.
- (8) Citry, O.; Baer, R.; Kosloff, R. *Surf. Sci.* **1996**, *351*, 24.
- (9) Raukema, A.; Butler, D. A.; Box, F. M. A.; Kleyn, A. W. *Surf. Sci.* **1996**, *347*, 151.
- (10) Kuznetsov, A. M. *Charge transfer in Physics, Chemistry and Biology*; Gordon & Breach: Reading (UK), 1995.
- (11) Bligard, T.; Nørskov, J. K.; Dahl, S.; Matthiesen, J.; Christensen, C. H.; Sehested, J. *J. Catal.* **2004**, *224*, 206.
- (12) Landau, L. D.; Lifshitz, E. M. *Quantum Mechanics*; Pergamon: Oxford, U.K., 1965.
- (13) Kuznetsov, A. M. *Stochastic and dynamic views of chemical reaction kinetics in solutions*; Presses polytechniques universitaires et romandes: Lausanne, 1999.